Fault-Tolerant Control of Autonomous Vehicles Using LPV-MPC and Direct Yaw Moment Compensation for Steering Failures

Mohamed Achraf Senoussi[1], Vicenç Puig[2], Mohamed Boumehraz[1], Chouki Sentouh[3] and Hossam Eddine Glida[4]

***Abstract*— This paper proposes a novel fault-tolerant control (FTC) reconfiguration strategy for autonomous vehicles using Model Predictive Control (MPC) based on a Linear Parameter Varying (LPV) model to address steering faults. The proposed approach compensates for the lack of redundant steering actuators by using force differences between the left and right sides of the vehicle to generate corrective yaw moments. By integrating both lateral and longitudinal dynamics, the MPC optimally allocates actuator efforts based on fault severity and desired speed. Simulation results validate the effectiveness of the proposed strategy in maintaining vehicle stability and performance under various fault scenarios, including complete steering failure, thereby ensuring safe autonomous operation.**

I. Introduction

Autonomous vehicles (AVs) have garnered significant attention in the research community, as they represent a transformative technology with the potential to revolutionize transportation in the near future. Ensuring the safety, efficiency, and reliability of AVs requires robust handling of various operational scenarios, including potential subsystem failures. Among these, the steering system is particularly critical, as faults in this mechanism can severely impact vehicle safety and stability. This highlights the importance of developing fault-tolerant control strategies to maintain safe and reliable autonomous driving, even in the presence of steering faults.

The literature contains extensive research on control strategies addressing steering faults in autonomous vehicles [1]–[5]. A significant challenge lies in the absence of redundant actuators for lateral control resulting in severe instability, compromising the vehicle safety and overall stability. One promising approach is Direct Yaw Moment (DYM) control, which introduces a corrective torque by creating a force difference between the right and left sides of the vehicle. This technique has been widely explored, primarily for improving vehicle lateral stability [6], [7], and it has also been used in FTC, where the corrective yaw moment compensates for steering loss during complete actuator failure [1], [2]. While this method has proven to be a robust alternative for maintaining vehicle lateral and yaw control, it introduces interference with longitudinal dynamics by applying braking forces or torques. This interference can lead to stability issues and performance degradation in overall longitudinal control. To address this challenge, researchers have proposed a two-stage control process in [3], the higher-level controller generates steering angles, driving forces, and yaw moments, while the lower-level controller distributes these forces and moments among the wheels.

Motivated by the above results, this paper proposes a unified control structure to address both longitudinal and lateral vehicle dynamics. The proposed approach integrates MPC with LPV modeling to generate steering efforts and wheel forces while accounting for steering faults and physical constraints. In this study, MPC is utilized not only to address the steering faults but also to optimize the generation of longitudinal forces. Unlike classical control allocation techniques [3], the proposed framework leverages MPC optimization capabilities to integrate the full vehicle dynamics, ensuring robust performance and stability under fault conditions. LPV modeling is developed to reduce computational complexity and address the challenges of nonlinear vehicle dynamics. To validate the effectiveness of the proposed methodology, extensive simulations are conducted under various operational scenarios, including steering actuator faults. The results demonstrate the ability of the control framework to maintain vehicle stability and achieve desired performance metrics. The main contributions of this paper can be outlined as follows:

- The full vehicle dynamics, encompassing longitudinal and lateral dynamics along with the direct yaw moment are formulated using LPV models. This approach reduces the computational burden, making the design feasible for real-time implementation within the MPC controller.
- The proposed methodology directly incorporates steering faults into the control design, eliminating the need for classical control allocation techniques. By optimizing wheel forces and steering efforts, the framework ensures vehicle stability and safety under faulty conditions.

[1]Mohamed Achraf Senoussi and Mohamed Boumehraz are with LI3CUB, University of Biskra, Algeria. e-mail: {achraf.senoussi,m.boumehraz}@univ-biskra.dz

[2]Vicenç Puig is with the Advanced Control Systems, Universitat Politècnica de Catalunya, Barcelona, Spain. e-mail: vicenc.puig@upc.edu

[3]Chouki Sentouh is with C. Sentouh is with LAMIH UMR-CNRS 8201, Hauts-de-France Polytechnic University and also with INSA Hauts-de-France, 59300 Valenciennes, France. e-mail: chouki.sentouh@uphf.fr

[4]Hossam Eddine Glida is with LIS UR 7478, University of Caen Normandie, ENSICAEN, UNICAEN, 14050 Caen, France. e-mail: hossam-eddine.glida@unicaen.fr

- Unlike conventional LPV-MPC schemes that simplify vehicle dynamics to a bicyle model controlled via steering angle and acceleration [8], we adopt a full four-wheel LPV representation that simultaneously captures both lateral and longitudinal couplings. This formulation enables independent control of left and right tire forces, offering redundant control control over vehicle direction.
- Unlike the strategies in [4], [5], which rely on predefined fault margins, the proposed strategy is capable of handling complete steering control loss. This is achieved through a reconfiguration mechanism that has been validated via simulation tests.

The rest of the paper is organized as follows: Section II outlines different parts of the vehicle dynamics. The control-oriented LPV model and fault integration are presented in Section III. Section IV discusses the formulations of MPC. Section V presents and discusses the results obtained from the simulation. Finally, Section VI concludes the paper by summarizing our findings and outlining potential future research directions.

II. Vehicle Model

This section represents both longitudinal and lateral vehicle dynamics assuming fault free steering system. It begins by introducing the nonlinear model. The second part of this section presents the interaction between the vehicle and the road, focusing on the lateral dynamics and the lane positioning error dynamics.

A. Dynamic Model

The equations of motion can be illustrated by studying the longitudinal speed v_x, lateral speed v_y and yaw rate ω, as shown in Fig. 1, which are given as [5]

$$\Sigma : \begin{cases} m\dot{v}_x &= (F_{x(fr)} + F_{x(fl)})\cos(\delta) + F_{x(rr)} + F_{x(rl)} \\ & \quad -F_{yf}\sin\delta + m\omega v_y \\ m\dot{v}_y &= (F_{x(fr)} + F_{x(fl)})\sin(\delta) + F_{yf}\cos(\delta) \\ & \quad +F_{yr} - m\omega v_x \\ I_z\dot{\omega} &= (F_{x(fr)} + F_{x(fl)})l_f\sin(\delta) + F_{yf}l_f\cos(\delta) \\ & \quad -F_{yr}l_r + \frac{d}{2}(F_{x(rr)} - F_{x(rl)}) \\ & \quad \frac{d}{2}(F_{x(fr)} - F_{x(fl)})\cos(\delta) \end{cases} \tag{1}$$

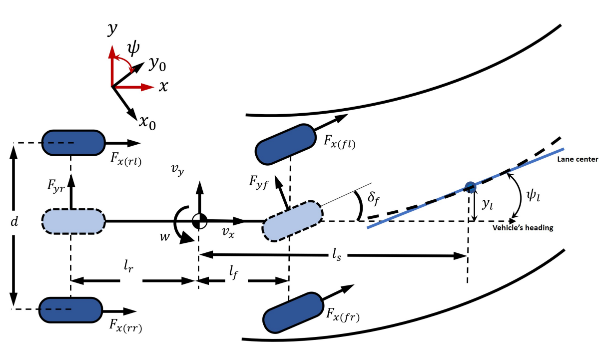

Fig. 1. Vehicle model configuration.

where δ is the steering control signal, m and I_z define the vehicle total mass and inertia around the z-axis, respectively, l_f and l_r are the distance from the vehicle center of gravity to the front and rear wheel axis, d is the car width, $F_{x(ji)}$ is the longitudinal tire forces where $j = \{f, r\}$ and $i = \{l, r\}$, F_{yf} and F_{yr} are the front and rear lateral tire forces, respectively, the lateral forces are represented by the following equations:

$$\begin{aligned} F_{yf} &= C_f\left(\delta - \frac{l_f\omega + v_y}{v_x}\right) \\ F_{yr} &= C_r\left(\frac{l_r\omega - v_y}{v_x}\right) \end{aligned} \tag{2}$$

where C_f and C_r are stiffness coefficients for the front and rear wheels. In this study, longitudinal tire dynamics are not considered since the longitudinal forces are directly used as control inputs for the system. From the vehicle dynamics, the yaw moment generated directly from differential longitudinal forces is

$$M_f = \frac{d}{2}(F_{x(fr)} - F_{x(fl)})\cos\delta + \frac{d}{2}(F_{x(rr)} - F_{x(rl)}) \tag{3}$$

This moment is independent of the vehicle steering actuator. Thus, it can be used as a redundant strategy to compensate for steering faults.

B. Vehicle-Road Model

Vehicle lane-keeping is achieved by analyzing the interaction between the vehicle and the road. This is done by defining the lateral deviation error y_l and the heading error ψ_l, both measured at a look-ahead distance l_p from the vehicle center of gravity [9]. The dynamics governing the vehicle position are expressed as

$$\begin{aligned} y_l &= y_c + l_s\sin(\psi_l) \\ \psi_l &= \psi - \psi_{des} \end{aligned} \tag{4}$$

where y_c is the lateral offset from the center of the vehicle. By deriving the above equations we find

$$\begin{aligned} \dot{y}_l &= v_y\cos\psi_l + v_x\sin\psi_l + l_s\dot{\psi}_l\cos\psi_l \\ \dot{\psi}_l &= \omega - \frac{v_x\cos\psi_l - v_y\sin\psi_l}{1 - y_l\kappa}\kappa \end{aligned} \tag{5}$$

where κ represents the road curvature.

III. Control Oriented Model including Faults

Actuator faults in AVs can have a significant impact on their performance and safety. Among these faults, steering faults are particularly critical as they directly influence the vehicle ability to maintain lane-keeping and trajectory tracking. The steering fault is modeled as a gain fault, which represents a loss of effectiveness (LOE) in the actuator, as follows:

$$\delta_f = f_\delta\delta \tag{6}$$

where δ_f represents the actual steering effort, f_δ defines the fault gain, assumed to be known, and δ denotes the desired steering generated by the controller. Consequently, $f_\delta = 1$ indicates a healthy actuator, while $f_\delta = 0$ corresponds to a complete failure.

Direct use of longitudinal forces as control inputs leads to scaling issues for MPC controller, as these forces can reach up to $24300\,N$, whereas the steering inputs and vehicle states operate within a much lower range. To address this issue, we propose normalizing the forces converting them into longitudinal accelerations for each wheel, achieved by dividing the forces by the vehicle mass, as follows:

$$a_{x(ji)} = \frac{F_{x(ji)}}{m} \tag{7}$$

On the other hand, the vehicle dynamics (1)-(5) are transformed into LPV model by embedding the non-linearities within varying parameters. This results in a linear-like model, where its matrices depend on the following scheduling variables:

$$\mathbf{\Gamma} = [v_x, v_y, y_l, \psi_l, \kappa, \delta] \tag{8}$$

This reformulation provides a model with linear structure what will allow reducing MPC computational complexity while maintaining high model accuracy. Therefore, the state-space matrices for the full LPV model, considering the steering fault and new inputs, are given as follows:

$$\begin{aligned} A(\mathbf{\Gamma}) &= \begin{bmatrix} 0 & A_{12} & A_{13} & 0 & 0 \\ 0 & A_{22} & A_{23} & 0 & 0 \\ 0 & A_{32} & A_{33} & 0 & 0 \\ A_{41} & A_{42} & l_p c(\psi_l) & 0 & 0 \\ -\frac{\kappa c(\psi_l)}{1-y_l\kappa} & \frac{\kappa s(\psi_l)}{1-y_l\kappa} & 1 & 0 & 0 \end{bmatrix} \\ B(\mathbf{\Gamma}) &= \begin{bmatrix} -\frac{C_f}{m}\boldsymbol{s}(f_\delta\delta) & \boldsymbol{c}(f_\delta\delta) & \boldsymbol{c}(f_\delta\delta) & 1 & 1 \\ \frac{C_f}{m}\boldsymbol{c}(f_\delta\delta) & \boldsymbol{s}(f_\delta\delta) & \boldsymbol{s}(f_\delta\delta) & 0 & 0 \\ \frac{l_f C_f}{I_z}\boldsymbol{c}(f_\delta\delta) & B_{32} & B_{33} & \frac{dm}{2I_z} & -\frac{dm}{2I_z} \\ 0 & 0 & 0 & 0 & 0 \\ 0 & 0 & 0 & 0 & 0 \end{bmatrix} \end{aligned} \tag{9}$$

The nominal parameters for the matrix $\boldsymbol{A}$ are detailed in Appendix A. Finally, considering the steering fault f_δ is given as follows:

$$\mathcal{SYS} : \dot{\boldsymbol{x}}(t) = A(\mathbf{\Gamma})\boldsymbol{x}(t) + B(\mathbf{\Gamma}) \underbrace{\begin{bmatrix} f_\delta & 0 & 0 & 0 & 0 \\ 0 & 1 & 0 & 0 & 0 \\ 0 & 0 & 1 & 0 & 0 \\ 0 & 0 & 0 & 1 & 0 \\ 0 & 0 & 0 & 0 & 1 \end{bmatrix}}_{\mathcal{F}_\delta} \boldsymbol{u}(t) \tag{10}$$

where $\boldsymbol{x} = [v_x, v_y, \omega, y_l, \psi_l]$ is the state vector and $\boldsymbol{u} = [\delta, a_{x(fr)}, a_{x(fl)}, a_{x(rr)}, a_{x(rl)}]$ is the control input vector.

IV. Active Fault-Tolerant Control Using LPV Modeling and Model Predictive Control

To achieve optimal control while considering steering faults and the vehicle physical limitations, an MPC controller is developed based on the presented LPV model. The controller is formulated as an optimal control problem with a quadratic cost function J and the LPV model in (10), resulting in a computationally efficient MPC as the following:

$$\min_{U_k, X_k} J = \sum_{i=1}^{N_{mpc}} \left(\|\boldsymbol{r}_{i|k} - \boldsymbol{x}_{i|k}\|^2_{\boldsymbol{Q}} + \|\boldsymbol{u}_{i|k}\|^2_{\boldsymbol{R}_u} + \|\Delta\boldsymbol{u}_{i|k}\|^2_{\boldsymbol{R}_{\Delta u}} \right) \tag{11}$$

where $\boldsymbol{r}_{i|k} = [v_x^{ref}, 0, 0, 0, 0]$ is the i^{th}-step ahead reference vector at time k, $\boldsymbol{x}_{i|k}$ and $\boldsymbol{u}_{i|k}$ are the i^{th}-steps ahead inputs and states predictions at time k, $\boldsymbol{x}_k$ is the state vector at the current time k, assuming to be known. The MPC optimization problem is subject to the following constraints:

$$\mathcal{M} : \begin{cases} \boldsymbol{x}_{i+1|k} &= \boldsymbol{A}_d(\mathbf{\Gamma}_{i|k})\boldsymbol{x}_{i|k} + \boldsymbol{B}_d(\mathbf{\Gamma}_{i|k})\mathcal{F}_\delta \boldsymbol{u}_{i|k} \\ \Delta\boldsymbol{u}_{i|k} &= \boldsymbol{u}_{i|k} - \boldsymbol{u}_{i-1|k} \\ \boldsymbol{u}_{i|k} &\in [\underline{\boldsymbol{u}}, \overline{\boldsymbol{u}}] \\ \boldsymbol{x}_{i|k} &\in [\underline{\boldsymbol{x}}, \overline{\boldsymbol{x}}] \\ \boldsymbol{x}_{1|k} &= \boldsymbol{x}_k \quad i = 1, ..., N_{mpc}+1 \end{cases}$$

where $\boldsymbol{A}_d$ and $\boldsymbol{B}_d$ are the discrete state space matrices using the Euler integration method, $\boldsymbol{Q}$, $\boldsymbol{R}_u$ and $\boldsymbol{R}_{\Delta u}$ are diagonal positive definite weighting matrices for tracking error, input efforts and input variation, respectively. The sets $[\underline{\boldsymbol{u}}, \overline{\boldsymbol{u}}]$ and $[\underline{\boldsymbol{x}}, \overline{\boldsymbol{x}}]$ include the vehicle inputs and state vector constraints based on their physical limitations.$U_k = [u_{1|k}, ..., u_{N_{mpc}+1|k}]$ and $X_k = [x_{1|k}, ..., x_{N_{mpc}+1|k}]$ are the set of predicted inputs and states. $\mathbf{\Gamma}_{i|k}$ represents the i^{th}-steps ahead scheduling vector at time k, where its values are derived from the previous optimization solution U_{k-1} and X_{k-1}.

The active fault-tolerant MPC formulation compensates for actuator degradation by incorporating the LOE gain f_δ into the model, which is updated at each controller sampling time through a fault estimation scheme that is not presented in this work. The MPC optimally redistributes control efforts to compensate for steering faults through two mechanisms:

1) Generating higher steering effort signals to compensate for LOE gain f_δ.
2) Generating a corrective yaw moment by introducing a force difference between the left and right wheels.

The MPC optimally determines the required actuation efforts to compensate for f_δ, considering both longitudinal control objectives and the steering actuator fault condition. This ensures the vehicle stability and performance under various fault scenarios.

V. Simulation Results

To evaluate the performance of the proposed fault-tolerant control strategy, simulations were conducted using the MATLAB/Simulink environment with Runge-Kutta integration and a sampling time of 0.001 seconds. The MPC controller was formulated with CasADi framework [10] and solved using Operator Splitting Quadratic Program solver. The MPC operates at a control frequency of $30Hz$ with a prediction horizon of $N_{mpc} = 15$ steps. The vehicle parameters used in the simulations are derived from the Sherpa vehicle model [5], and the "Satory" test track trajectory is employed with predefined longitudinal velocity and road curvature. The fault is assumed to be known and is directly injected into the

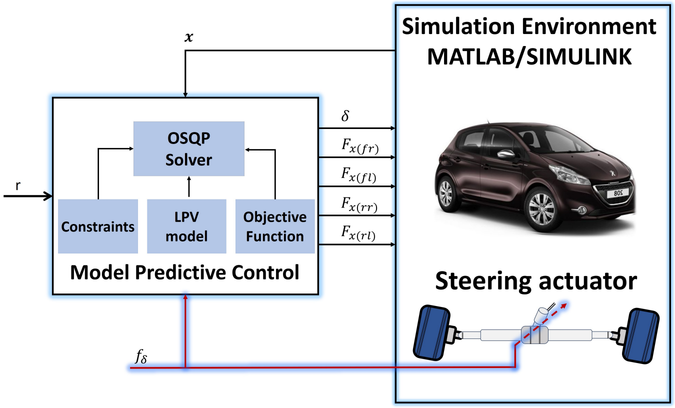

Fig. 2. The proposed methodology of the vehicle control.

vehicle steering system and MPC, where it is updated at each iteration. Fig. 2 illustrates the simulation setup.
Two simulation scenarios are considered to demonstrate the effectiveness of the proposed FTC as the following.

A. Scenario 1: Loss of steering actuator effectiveness

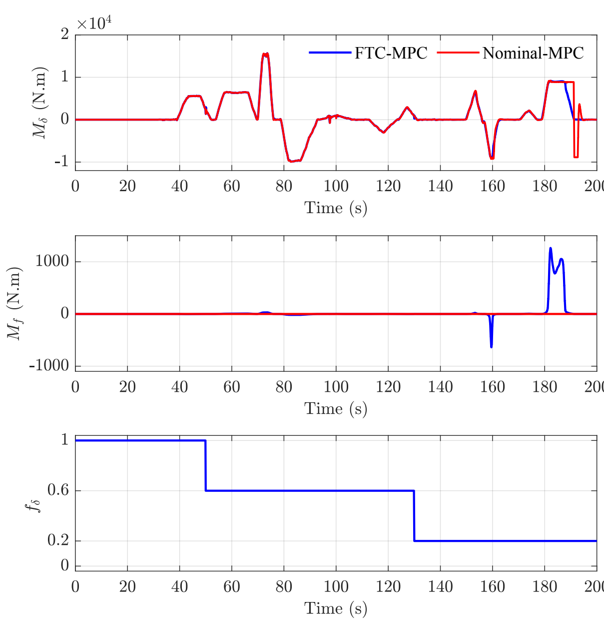

Fig. 3. Scenario 1: generated moments.

In this scenario, partial loss of steering actuator effectiveness is introduced during the simulation to assess the controller ability to compensate for degraded steering performance. The variation of LOE gain is presented in Fig. 3, where this gain is firstly reduced to $f_\delta = 0.6$ at $t = 50s$, followed by a second degradation to $f_\delta = 0.2$ (80% efficiency loss) at $t = 130s$. Additionally, in this figure, the proposed FTC scheme is compared with nominal LPV-MPC that does not consider actuator faults and lacks the capability to generate direct yaw moments.

Fig. 4 presents the vehicle different states for the first simulation. During the initial fault ($f_\delta = 0.6$), both the nominal MPC and the proposed FTC-MPC successfully maintained vehicle stability, with the FTC-MPC demonstrating minor performance advantages. However, as the steering effectiveness is further degraded to $f_\delta = 0.2$, the nominal MPC failed to maintain control, resulting in a lateral deviation of up to $3m$, which is unacceptable in real-world scenarios. In contrast, the FTC-MPC maintained accurate trajectory tracking despite the severe degradation. This superior performance is attributed to the integration of the fault into the controlling model, which enables the FTC-

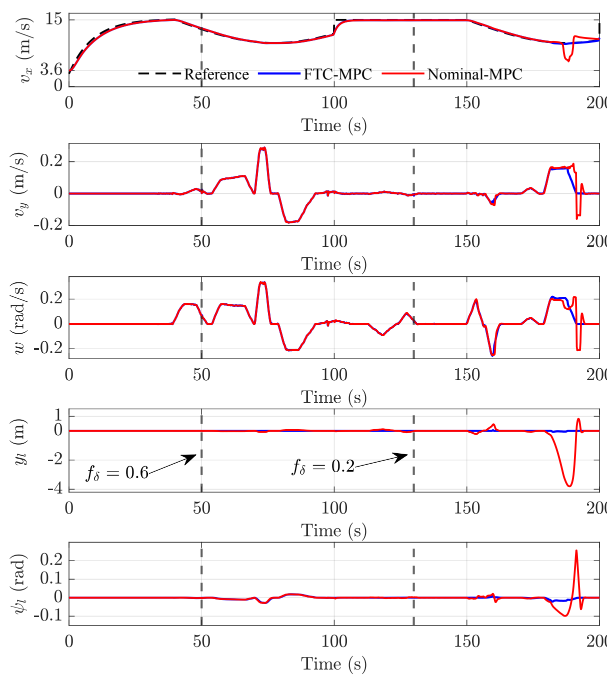

Fig. 4. Scenario 1: Vehicle States.

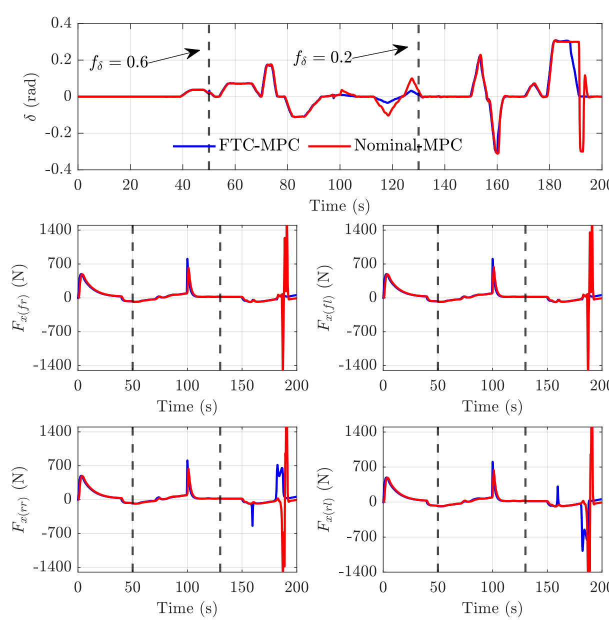

Fig. 5. Scenario 1: Control inputs.

MPC to account for actuator degradation and adapt its control strategy accordingly. Fig. 5 illustrates the control forces generated by both controllers. For the initial fault ($f_\delta = 0.6$), similar control forces were observed from both controllers, demonstrating the natural fault tolerance of nominal MPC for small faults without prior knowledge. However, under severe degradation ($f_\delta = 0.2$), the steering actuator is saturated and is no longer able to generate the proper effort to control the system. For that, the FTC-MPC effectively compensated for the fault by generating differential longitudinal forces between the rear wheels. Conversely, the nominal MPC generated very aggressive signals, which may be impractical for real-world implementation and could potentially damage the actuators.

To further study the effect of the redundant actuator, Fig. 3 shows the moments generated by both the steering system $M_\delta = f_\delta \delta \frac{l_f C_f}{I_z} cos\left(f_\delta \delta\right)$ and the direct yaw moment in (3). Both controllers exhibited comparable steering moment profiles, with minor deviations observed in the final turn, where the nominal MPC applied an aggressive steering correction, which led to the high lateral deviation discussed before. However, FTC-MPC generated a direct yaw moment to complement the steering moment in the last turn, where the steering actuator suffered severe degradation and saturation. The results also show that the FTC-MPC prioritizes fault compensation by primarily increasing steering efforts, only resorting to differential braking when the steering actuator reaches its saturation limits. This approach is beneficial for the longitudinal dynamics control.

B. Scenario 2: Complete failure of the steering actuator

The second scenario evaluates the ability of the direct yaw moment control to stabilize the vehicle in the event of complete steering failure ($f_\delta = 0$), when we introduce the fault at $t = 40s$.

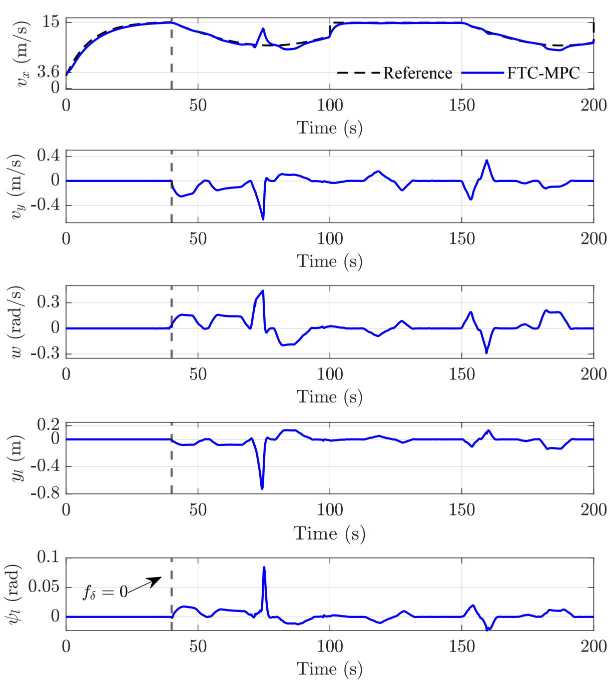

Fig. 6. Scenario 2: Vehicle States.

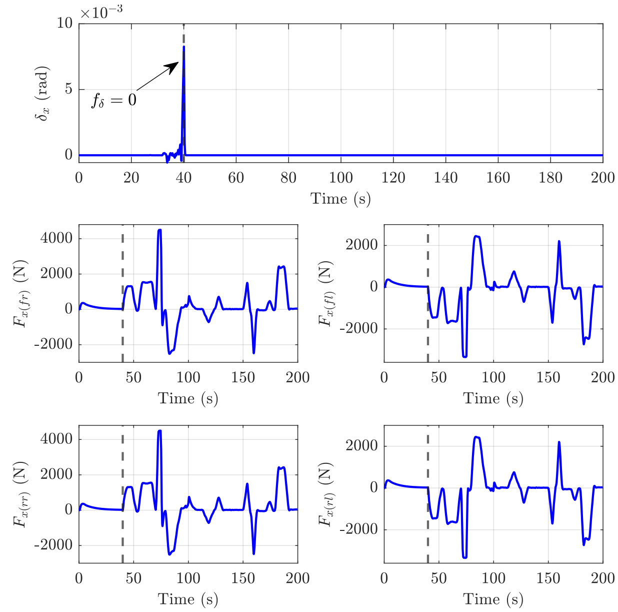

Fig. 7. Scenario 2: Control inputs.

Fig. 6 presents the state of the vehicle, demonstrating that the controller successfully maintained stability and trajectory tracking despite the total loss of steering control. A noticeable peak occurs at $t = 70s$ due to an aggressive turn in the "Satory" test track trajectory. However, the lateral error remained within an acceptable range of 0.8 meters and the vehicle quickly returned to its intended path, confirming the effectiveness of the controller even in challenging conditions. In addition, the controller ensured longitudinal stability despite using longitudinal forces for vehicle orientation. Fig. 7 illustrates the control inputs, showing that the steering system was completely disabled after the fault occurrence. At this point, the controller began to generate opposing longitudinal forces between the right and left wheels to create the necessary yaw moment and maintain stability. Without steering input, the controller relied solely on differential braking to manage vehicle orientation. Despite aggressive trajectory, high speed ($v_x = 15m/s$), and complete steering failure, the FTC-MPC generated a smooth signal in acceptable ranges, while reaching the limits at $t = 70s$ which corresponds to the aggressive turn we discussed earlier.

To further analyze control efforts, Fig. 8 displays the torque generated by different control strategies. It confirms that the steering system was deactivated after the fault occurred. Unlike the first scenario, the corrective yaw torque increased significantly to compensate for the steering loss. Interestingly, the generated yaw torque is similar to the steering torque observed in the first scenario (Fig. 3), indicating the effectiveness of the proposed strategy as a redundant strategy to replace the steering actuator.

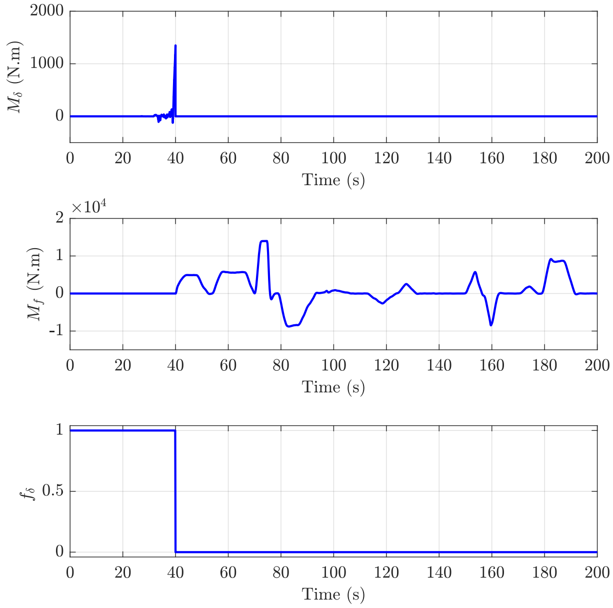

Fig. 8. Scenario 2: generated moments.

VI. CONCLUSIONS

This paper presented a fault-tolerant control strategy for autonomous vehicles using an LPV-based MPC approach to address steering actuator failures. The approach compensates for steering faults by generating corrective yaw moments, ensuring vehicle stability and trajectory tracking. By integrating both lateral and longitudinal dynamics, the strategy optimally allocates actuator efforts based on fault severity and driving conditions. Simulation results showed that the FTC-MPC strategy effectively handled various fault scenarios, outperforming the nominal MPC, which failed under severe faults. The proposed approach maintained stability by relying on the steering system and corrective yaw moments when necessary. Future work will focus on experimental validation using the LAMIH full-scale SHERPA driving simulator and extending the framework to include real-time fault detection and estimation.

APPENDIX

A. Linear Parameter-Varying Model With Steering Fault

Consider the LPV model represented in (10). The following nominal parameters for the system are then defined as:

$$
\begin{aligned}
A_{12} &= \frac{\boldsymbol{s}\left(f_\delta \delta\right) C_f}{m(v_x+\epsilon)} \qquad & A_{13} &= \frac{s(f_\delta * \delta) C_f l_f}{m(v_x+\epsilon)} + v_y \\
A_{22} &= -\frac{C_r + C_f \boldsymbol{c}\left(f_\delta \delta\right)}{m(v_x+\epsilon)} \qquad & A_{23} &= \frac{l_r C_r - l_f C_f \boldsymbol{c}\left(f_\delta \delta\right)}{m\left(v_x+\epsilon\right)} - v_x \\
A_{32} &= \frac{l_r C_r - l_f C_f \boldsymbol{c}\left(f_\delta \delta\right)}{I_z\left(v_x+\epsilon\right)} \qquad & A_{33} &= -\frac{l_f^2 C_f \boldsymbol{c}\left(f_\delta \delta\right) + l_r^2 C_r}{I_z\left(v_x+\epsilon\right)} \\
A_{41} &= \boldsymbol{s}\left(\psi_l\right) - \frac{\boldsymbol{c}\left(\psi_l\right)^2 \kappa l_s}{1 - y_l \kappa} \qquad & A_{42} &= \boldsymbol{c}\left(\psi_l\right) + \frac{\boldsymbol{s}\left(\psi_l\right) \kappa l_s}{1 - y_l \kappa} \\
B_{32} &= \frac{l_f m}{I_z} \boldsymbol{s}\left(f_\delta \delta\right) + \frac{dm}{2 I_z} \cos\left(f_\delta \delta\right) & & \\
B_{33} &= \frac{l_f m}{I_z} \boldsymbol{s}\left(f_\delta \delta\right) - \frac{dm}{2 I_z} \cos\left(f_\delta \delta\right) & &
\end{aligned}
\tag{12}
$$

ACKNOWLEDGMENT

The authors acknowledge the support of the University of Biskra, the Algerian Ministry of Higher Education and Scientific Research, the French Ministry of Higher Education and Research and the French National Center for Scientific Research. This work has been co-financed by the Spanish State Research Agency (AEI) and the European Regional Development Fund (ERFD) through the project SaCoAV (ref. MINECO PID2020-114244RB-I00)

REFERENCES

[1] J. Wang, Q. Wang, L. Jin, and C.-x. Song, "Independent wheel torque control of 4wd electric vehicle for differential drive assisted steering," *Mechatronics*, vol. 21, no. 1, pp. 63–76, 2011.

[2] C. Hu, R. Wang, F. Yan, and H. R. Karimi, "Robust composite nonlinear feedback path-following control for independently actuated autonomous vehicles with differential steering," *IEEE Transactions on Transportation Electrification*, vol. 2, no. 3, pp. 312–321, 2016.

[3] Y.-H. Ji and Y.-C. Liu, "Force allocation control for distributed drive electric vehicles under split-friction regions and actuator faults," *ISA transactions*, vol. 129, pp. 398–412, 2022.

[4] H. E. Glida, C. Sentouh, A. Chelihi, J. Floris, and J.-C. Popieul, "Event-triggered adaptive fault-tolerant control based on sliding mode/neural network for lane keeping assistance systems in steer-by-wire vehicles," *IEEE Transactions on Intelligent Vehicles*, 2024.

[5] C. Sentouh, M. Fouka, J. J. Rath, and J.-C. Popieul, "Adaptive observer-based output feedback ftc for nonlinear interconnected vehicle dynamics with unknown actuator faults," *IEEE Transactions on Intelligent Vehicles*, 2024.

[6] R. Hajiloo, A. Khajepour, A. Kasaiezadeh, S.-K. Chen, and B. Litkouhi, "A model predictive control of electronic limited slip differential and differential braking for improving vehicle yaw stability," *IEEE Transactions on Control Systems Technology*, vol. 31, no. 2, pp. 797–808, 2022.

[7] H. Zhang, K. Xv, Y. Li, W. Zhao, and C. Wang, "Coordination control strategy of motion stability and tire slip for electric vehicle driven by in-wheel-motors," *Journal of the Franklin Institute*, vol. 361, no. 15, p. 107126, 2024.

[8] E. Alcalá, V. Puig, and J. Quevedo, "Lpv-mpc control for autonomous vehicles," *IFAC-PapersOnLine*, vol. 52, no. 28, pp. 106–113, 2019.

[9] H. E. Glida, M. R. Oudainia, C. Sentouh, and J.-C. Popieul, "A new model-free shared control for lane-keeping assist system: theory and experimental validation," *IEEE Transactions on Intelligent Vehicles*, 2024.

[10] J. A. Andersson, J. Gillis, G. Horn, J. B. Rawlings, and M. Diehl, "Casadi: a software framework for nonlinear optimization and optimal control," *Mathematical Programming Computation*, vol. 11, pp. 1–36, 2019.